Diminished gap junction coupling under diabetogenic conditions does not drive loss of functional β-cell sub-populations

Claire H Levitt[a], Dominic Isaacs[a], Maria S Hansen[b], Vira Kravets[a], Jennifer K Briggs[a], Richard KP Benninger[a,b,1]

[a] Department of Bioengineering, University of Colorado, Anschutz Medical campus, Aurora, CO. USA

[b] Barbara Davis center for childhood diabetes, University of Colorado, Anschutz Medical campus, Aurora, CO. USA

[1] To whom correspondence should be addressed: richard.benninger@cuanschutz.edu Tel: (303) 724-6388. Fax: (303) 724-5800.
1775 Aurora court, M20-4306D, mailstop B140, University of Colorado Anschutz Medical campus, Aurora, CO. 80045.

Running Title: β-cell sub-populations under diabetogenic conditions

Key Words: Optogenetics, Islet Dynamics; Optical Microscopy; Diabetes; Gap junctions

Classification: Systems Biology

Manuscript word count: 4432
Abstract word count: 272
Number of figures: 4

Abstract

Within the islets of Langerhans, gap junction coupling is important for synchronizing oscillatory free-calcium activity ([Ca^{2+}]) and regulating pulsatile insulin release. In islets from multiple models of diabetes, gap junction coupling is disrupted, and [Ca^{2+}] synchronization and pulsatile insulin is lost. Functional sub-populations have been identified within the islet that are linked to driving synchronized [Ca^{2+}] and insulin release. These sub-populations can be disrupted under conditions associated with diabetes such as glucolipotoxicity and inflammatory environments, and their loss may drive islet dysfunction. Here we investigate how loss of gap junction coupling influences functional subpopulations under diabetogenic environments. We treated islets with a cocktail of pro-inflammatory cytokines and specifically recovered gap junction coupling via co-treatment with a Cx36 mimetic peptide S293 that was previously shown to protect gap junction permeability and synchronized [Ca^{2+}] dynamics. We performed calcium imaging and ChR2 stimulation, analyzed islet [Ca^{2+}] dynamics and the presence of functional sub-populations including hubs and first-responders. 1h or 24h cytokine-treatment disrupted gap junction coupling, which was fully recovered by S293 peptide co-treatment. Treatment with pro-inflammatory cytokines decreased the recruitment of [Ca^{2+}] upon ChR2 stimulation, increased the time between first and last responding cells upon glucose stimulation, and reduced the number and consistency of hub cells. When preserving gap junction coupling by S293 during cytokine treatment, the presence and consistency of these sub-populations was only marginally improved. We therefore concluded that restoration of gap junctions alone is not sufficient to recover functional sub-populations and their influence over islet function upon diabetogenic conditions associated with diabetes. Thus, preventing a disruption to intrinsic β-cell properties that define functional subpopulations is likely important for preserving these sub-populations during diabetes.

52 ***Introduction***

53 Diabetes Mellitus (DM) affects approximately 537 million people globally [1,2], and is
54 characterized by the dysfunction and/or death of insulin-secreting β-cells in the islets of
55 Langerhans in the pancreas. β-cells in the islet secrete insulin in response to elevations in
56 blood glucose or other nutrients. At elevated glucose, β-cells show increased ATP/ADP
57 following the metabolism of glucose, which drives membrane depolarization via closure of ATP-
58 sensitive K+ (K_{ATP}) channels and activation of voltage gated calcium (Ca_V) channels.
59 Subsequent oscillations of intracellular free-calcium ([Ca^{2+}]) across the islet drive the release
60 of insulin in discrete pulses.

61 The dynamics of [Ca^{2+}] are synchronized across β-cells in the islet, which is facilitated
62 by connexin-36 (Cx36) gap junctions [3-5]. Gap junctions synchronize the β-cell response to
63 glucose despite heterogeneity in β-cell metabolism and excitability [6,7]. Under low glucose
64 conditions, gap junction-mediated hyper-polarizing currents suppress spontaneous elevations
65 in [Ca^{2+}] from excitable β-cells [8,9]. At high glucose, gap junction-mediated depolarizing
66 currents coordinate both first-phase [Ca^{2+}] and oscillatory second phase [Ca^{2+}] responses [3].
67 In Cx36 knockout models, synchronous [Ca^{2+}] responses are disrupted [3,5,9], both first phase
68 insulin secretion and second phase insulin pulses are diminished and glucose tolerance is
69 impaired [5,10]. Importantly, islet gap junction coupling is disrupted under conditions associated
70 with diabetes including by glucolipotoxicity [2,11,12] and pro-inflammatory cytokines [13] as
71 well as in mouse models of diabetes [14-16] and human [11,12,17]. Synchronous [Ca^{2+}] activity
72 is also disrupted under conditions associated with diabetes [11,13,17,18] likely as a result of
73 disrupted Cx36 gap junction coupling.

74 β-cells are heterogeneous in gene expression [19-21], glucose sensitivity [6,19], insulin
75 secretion [22], and cell-to-cell communication [23]. As a result, β-cells exhibit functional
76 heterogeneity, and display distinct insulin secretory patterns. Previous studies found that ~75%
77 of β-cells exhibited a fixed response to glucose and ~25% fluctuated between states of
78 responsive and unresponsiveness [24]. The characterization of β-cell heterogeneity has led to
79 the identification of functional subpopulations which are thought to play distinct roles in
80 governing the spatiotemporal [Ca^{2+}] and insulin secretory dynamics of the islet [25,26]. For
81 example, following optogenetic ChR2 stimulation, a population of β-cells can recruit and
82 elevate [Ca^{2+}] in a large number of neighboring β-cells within the islet [27]. Similarly, 'first-
83 responder cells', that are first to show elevated [Ca^{2+}] upon elevated glucose stimulation, can

recruit and coordinate less excitable cells to respond earlier [28]. This first-responder subpopulation is distinct from previously identified ‘hub cells’ that exhibit a high degree of co-activity with neighboring β-cells [29] and have been shown to play a critical role in driving the synchronized oscillatory dynamics. Importantly, upon both glucolipotoxic environments and pro-inflammatory cytokines, the proportion of highly connected ‘hub cells’ declines [29]. This finding suggests that a selective loss of functional sub-populations may be sufficient to drive islet dysfunction in diabetes. However, the mechanisms underlying this loss of cells are unclear.

In this study, we seek to understand how functional sub-populations of cells are disrupted under conditions associated with diabetes. We specifically ask whether the loss of gap junction coupling that is associated with diabetes is a primary cause for the loss of these sub-populations and their influence over islet function. We first test how functional sub-populations are influenced by pro-inflammatory cytokine treatment. We then test for a role of gap junction coupling, by using a Cx36 mimetic peptide [12] that was previously shown to specifically protect gap junction permeability and retain glucose-stimulated [Ca^{2+}] dynamics under conditions associated with diabetes.

100 ***Materials and Methods***

101 *Mice/Animal Care:* Islets expressing ChR2-YFP in β-cells was achieved by crossing Pdx^{PB}-Cre
102 (Jackson Laboratory) and ROSA26-lox-STOP-lox-ChR2-YFP mice (Jackson Laboratory).
103 Islets expressing GCaMP6s in β-cells was achieved by crossing MIP-Cre^{ER} mice (Jackson
104 Laboratory) and ROSA26-lox-STOP-lox-GCaMP6s mice (Jackson Laboratory). Mice were
105 genotypes via qPCR (Transnetyx). All animal experiments were approved by the University of
106 Colorado Institutional Animal Care and Use Committee (IACUC Protocol number: 000024).
107 Mice were housed in a temperature-controlled environment with a 12 hr light/dark cycle and
108 continuous access to both food and water. For mice with β-cell specific GCaMP6s expression,
109 tamoxifen (solubilized in corn oil) was administered via IP injection for 5 consecutive days (50
110 mg/kg of body weight) to facilitate CreER-mediated recombination.
111
112 *Islet Isolation and Culture:* Islets were isolated from mice under ketamine/xylazine anesthesia
113 and euthanized via exsanguination. Collagenase (Type V, Sigma) was delivered to the
114 pancreases at a concentration of 2.5 mg/mL via the bile duct. After inflation, the pancreas was
115 surgically removed and digested (5 min at 37 °C). Islets were then hand-picked and cultured in
116 RPMI medium (Gibco) containing 10% fetal bovine serum, 100 U/mL penicillin, 100 ug/mL
117 streptomycin, and 11 mM glucose. Islets were incubated at 37°C, 5% CO2.
118
119 *Islet Treatment:* Islets were treated overnight with a '0.1x' cocktail of proinflammatory cytokines
120 (5 ng/mL IL-1β , 10 ng/mL TNF-α, and 100 ng/mL IFN-γ), as previously used [13] To restore
121 gap junction coupling, islets were co-treated with 30 μM mimetic peptide S293 for 1-6 hours for
122 experiments using optogenetic stimulation, and 24 hours for experiments measuring gap
123 junction permeability (FRAP) and calcium activity ([Ca^{2+}]).
124
125 *Fluorescent Recovery After Photobleaching and Analysis* Gap junction permeability was
126 assessed by Fluorescence Recovery After Photobleaching (FRAP) [4]. Isolated islets were
127 immobilized onto glass bottom dishes (MatTek) using cell tissue adhesive (CellTak, Corning)
128 and incubated at 37°C, 5% CO2 overnight. Islets were then loaded with 12.5 mM cationic dye
129 Rhodamine-123 for 30 minutes at 37°C in Hank's Balanced Salt Solution (HBSS) at 5mM
130 glucose. Islets were washed and imaged at room temperature in HBSS using a Zeiss LSM 800
131 confocal microscope with a x40 1.2NA water immersion objective. Rhodamine-123 was excited

132 at 488 nm. Half the islet area was selected using a rectangular ROI and photobleached for 25
133 frames at 40% laser power and achieved ~50% bleaching on average. Images were collected
134 every 5 seconds for 6 to 10 minutes.

135 Image analysis of Rh123 dye diffusion after photobleaching was conducted using
136 MATLAB and Image J. Fluorescent recovery was measured within a region of interest
137 encompassing the entire photobleached area and individual cells. The initial fluorescence
138 intensity was considered the point directly after photobleaching (I_P). Fluorescence recovery
139 was the final fluorescence (I_F) once the diffusion of dye reached a plateau. The recovery was
140 calculated as a percentage, relative to the initial intensity before photobleaching (I_0) as follows:

141 $$\%\ Recovery = 100 * \frac{I_F - I_P}{I_0 - I_P}$$

142 The rate of fluorescent recovery was calculated based on the linearized exponential fluorescent
143 recovery curve of the bleached area over time (I_i) normalized to the total recovery. Calculations
144 were conducted as follows:

145 $$Rate\ of\ recovery = -Ln(1 - \frac{I_i - I_P}{I_0 - I_P})$$

146

147 *Channelrhodopsin-2 Single Cell Entrainment and Analysis:* ChR2-YFP expressing islets were
148 incubated with pro-inflammatory cytokines, with or without S293 mimetic peptide, or S293
149 peptide alone for 6 hours after isolation in RPMI medium (Gibco) containing 10% fetal bovine
150 serum, 100 U/mL penicillin, 100 ug/mL streptomycin, and 11 mM glucose at 37°C, 5% CO2
151 prior to study.

152 Islets were loaded with 2μM of calcium indicator Rhodamine-2 (Rhod-2) in BMHH
153 imaging solution (125mM NaCl, 5.7mM KCl, 2.5mM CaCl2, 1.2mM MgCl2, 10mM HEPES,
154 2mM glucose, and 0.1% BSA, pH 7.4) for 35 minutes at 37°C. Islets were then washed and
155 imaged on a glass bottom dish in a 5mM glucose imaging solution using a LSM 800 confocal
156 microscope kept at 37°C .

157 ChR2-YFP was excited at 488 nm. A rectangular ROI was drawn within the bounds of a
158 single cell, so as to avoid stimulating neighboring cells that express ChR2-YFP. The cell was
159 activated using a photobleaching macro (intensity 5% laser power) for 8 stimulations at a
160 frequency of 0.1 Hz. Rhod-2 was simultaneously excited at 560 nm and the corresponding Ca^{2+}
161 response across the whole islet was measured based on fluorescent intensity of Rhod-2 that
162 was coincident to ChR2 stimulation.

163 MATLAB was used to analyze Channelrhodopsin-2 recruitment data, as previously
164 described [27]. Islets were selected by hand drawing a region of interest around the islet.
165 Background was identified as regions that did not show any calcium response. Activity was
166 based on the fluorescent intensity of the Ca^{2+} indicator Rhod-2 upon ChR2 stimulation and
167 assessed using individual pixel time-courses. A pixel was considered 'active' if its intensity was
168 twice that of the background. A threshold of 0.15 was used to determine which regions of the
169 islet were activate due to ChR2 stimulation compared to the islet average. The percent of the
170 islet area that was 'active' was calculated as a proportion of the entire islet area.
171
172 *GCaMP6 Imaging of Calcium Dynamics and Analysis:* Isolated islets expressing β-cell specific
173 GCaMP6 were incubated overnight with proinflammatory cytokines with or without S293
174 mimetic peptide, or S293 peptide alone. 30 minutes prior to imaging, islets were fasted at 2mM
175 glucose in BMHH imaging solution. Islets were then transferred to a glass bottom dish and
176 imaged on an LSM 800 confocal microscope. GCaMP6 fluorescence was excited at 488 nm
177 with images collected at 1 frame/sec for approximately 80 minutes. 3-5 minutes after the start
178 of imaging, glucose was raised from 2mM to 11mM. For experiments measuring consistency
179 between first responders and hub cells, glucose was subsequently lowered to 2mM after
180 achieving second phase oscillations for 10-15 minutes. After the islet had returned to basal
181 activity without oscillations (~15 minutes), the glucose concentration was increased again to
182 11mM. Samples were imaged at either x20NA or x40NA water immersion and held at 37°C.
183 Calcium dynamics were analyzed using MATLAB, first phase response time,
184 identification of first and last responders, and characterization of highly connected hub cells
185 was determined as previously described [28]. Briefly, to identify the response time, we
186 determined the time at which individual β-cells reached their half maximum amplitude following
187 stimulation from low to high glucose. This response time was rank ordered for all cells in the
188 islet. The earliest 10% were classed as first responders and the latest 10% classed as last
189 responders. ΔT was calculated as the difference in time between the means of the last
190 responders and first responders. The percent consistency was determined as a proportion of
191 first 5 responding cells of the initial stimulation that were also first responders during repeated
192 stimulation.
193 Highly correlated β-cell cells were identified using the calcium time-course of the high
194 glucose second phase. A highly correlated β-cell is a β-cell whose calcium activity strongly

195 parallels many other β-cell in the islet. To quantify the degree of correlation, the cross-
196 correlation value obtained using the xcorr function in MATLAB across all measured β-cell
197 calcium time traces was compared among each cell. “Links” were derived using a threshold of
198 correlation above 0.9. The top 60% of linked cells were considered hubs, (as defined in [Cite
199 Johnston et al].
200
201 *Statistical analysis:* 2-sided t-test was used to compare 2 groups, whereas ANOVA with
202 Tukey’s multiple comparisons test was used to compare multiple treatment groups, where *
203 indicates $p < 0.05$, ** indicates $p < 0.01$, *** indicates $p < 0.001$, **** indicates $p < 0.0001$.
204

205 ***Results***

206 *Successful restoration of gap junction coupling by Cx36 S293 mimetic peptide under pro-*
207 *inflammatory cytokines:* To test whether functional sub-populations are disrupted by a cocktail
208 of pro-inflammatory cytokines (0.5 ng/mL IL1-β, 1 ng/mL TNF-α, and 10 ng/mL IFN-γ), and
209 whether sub-population loss depends on loss of gap junction coupling, we followed an
210 approach outlined in Figure 1A. To assess gap junction permeability and confirm a disruption
211 to gap junction coupling by pro-inflammatory cytokines and recovery by S293 mimetic peptide
212 we used FRAP (Figure 1.B), as previously established [4]. Islets treated with pro-inflammatory
213 cytokines showed a reduction in gap junction permeability, as indicated by a slower recovery
214 rate. During co-treatment with the S293 mimetic peptide islets showed a significant increase in
215 the recovery rate compared to cytokine treatment alone (Figure 1.C, $p = 0.0471$). No significant
216 difference was observed between untreated control and co-treatment groups ($p = 0.9958$) or
217 untreated control vs S293 mimetic peptide alone ($p = 0.9979$). Thus co-treatment with S293
218 peptide fully restores gap junction permeability, consistent with previous studies that use the
219 S293 mimetic peptide to specifically recover gap junction coupling in diabetogenic
220 environments [12].
221
222 *Restoration of gap junction coupling provides a partial recovery to the cytokine-mediated*
223 *disruption of ChR2-mediated recruitment of [Ca^{2+}]:* With the conditions established to restore
224 gap junction coupling under a diabetogenic environment, we asked whether functional
225 subpopulations of β-cells are also restored.. Previous studies applied the optogenetic construct
226 ChannelRhodopsin-2 (ChR2) and single cell stimulation to discover a subpopulation of β-cells
227 with elevated metabolic activity that can recruit large numbers of neighboring cells when
228 activated [27]. We therefore first examined how pro-inflammatory cytokines influenced these
229 sub-populations and then tested the effects of gap junction coupling restoration on these sub-
230 populations.
231 Islets from $Pdx1^{PB}$-Cre;Rosa-LSL-ChR2-YFP mice that express ChR2 in β-cells were
232 loaded with the Ca^{2+} dye Rhod2. ChR2 expressing cells were subjected to focal stimulation in
233 single β-cells and the spatial Ca^{2+} response was observed in neighboring cells (Figure 2.A).
234 We quantified the proportion of β-cells in the imaging plane that showed Ca^{2+} elevations
235 coincident with ChR2 stimulation. This was repeated in ChR2-expressing islets treated with a
236 cocktail of pro-inflammatory cytokines (Figure 2.B) and/or Cx236 S293 peptide mimetic.

237 Under all treatments we observed heterogeneity in the recruitment of elevated [Ca^{2+}]
238 following single cell stimulation (Figure 2.C). In untreated control islets, on average ~42% of
239 cells within the imaging plane showed elevated [Ca^{2+}] following single cell stimulation, with a
240 substantial variation (Figure 2.C,D) as previously observed [27]. Treatment with pro-
241 inflammatory cytokines (for 1 hour) led to a significant decrease in the proportion of cells
242 showing elevated [Ca^{2+}] following single cell stimulation (~15%) compared to untreated controls
243 ($p < 0.0001$, Figure 2.C,D). Co-treatment with the S293 mimetic peptide led to a moderate
244 increase in elevated [Ca^{2+}] following single cell stimulation (~25%) (Figure 2.C,D), however this
245 was still significantly lower than in untreated control ($p = 0.0026$). Treatment with S293 peptide
246 alone showed a similar proportion of cells with elevated [Ca^{2+}] (~35%) to untreated control
247 islets (Figure 2.C,D).
248 Untreated control islets showed broad heterogeneity in the recruitment of [Ca^{2+}] (Figure
249 2.C), as previously observed [27]. This included a population of cells that recruited elevated
250 [Ca^{2+}] across the median recruited area of the untreated control islet (>30%, Figure 2.C), as
251 also previously observed [27]. Under cytokine treated (1 hour), this 'high recruiting' population
252 of cells was almost completely absent (~4%, Figure 2.E). Co-treatment with S293 mimetic
253 peptide partially recovered this population of cells (~10%, Figure 2.E), but again much less
254 than in either untreated controls or S293 peptide treatment alone.
255 Therefore, treatment with pro-inflammatory cytokines reduced the ChR2-mediated
256 recruitment of cells to increase [Ca^{2+}], with an abolishment of 'high-recruiting' cells. Restoration
257 of gap junction coupling only partially restored ChR2-mediatred recruitment of cells to increase
258 [Ca^{2+}] with only a small recovery of 'high-recruiting' cells.
259
260 *Restoration of gap junction coupling does not recover the cytokine-mediated disruption to first*
261 *responder cells and the 1st phase [Ca^{2+}] response:* We next examined the impact of pro-
262 inflammatory cytokines and the restoration of gap junction coupling on first responder cells and
263 the first phase [Ca^{2+}] response. Islets from β-cell specific GCaMP6 mice were used to assess
264 changes in [Ca^{2+}] following glucose elevation. We measured the [Ca^{2+}] response of individual
265 cells and ranked their response time after glucose stimulation. First responder cells were
266 identified as the 10% of cells which showed the earliest response, and last responders as the
267 10% of cells that showed the latest response, with the spread in response time (Δt) being the
268 time between first and last responders (Figure 3.A). In control untreated islets the response

269 time was fairly narrow (Δt=175s). Upon treatment with pro-inflammatory cytokines for 1 hour,
270 there was no significant impact on the time between first and last responders (Figure 3.A-B).
271 However following treatment with pro-inflammatory cytokines for 24 hours there was a
272 significant increase in the time between first and last responders (Δt=380s) compared to
273 untreated control islets (p=0.0036, Figure 3.A-B). Using this 24 hour treatment, co-treatment
274 with S293 peptide did not show a decrease in Δt compared to cytokines alone, indicating
275 restoration of gap junction coupling was not sufficient to recover the narrow spread of the first
276 phase response (Figure 3.C). S293 peptide alone showed a similar time between first and last
277 responders as untreated controls. Under 1 hour cytokine treatment, co-treatment with S293
278 had no impact (Supplemental 1).

279 Clusters of first responders were previously found to be consistent upon repeated
280 glucose stimulations [28]; where ~35% of first responder cells remained first responders and
281 ~75% of first responders remained within a 1 cell distance separation. We tested whether this
282 consistency was affected by both pro-inflammatory cytokines and restoration of gap junction
283 coupling. We identified the first 5 responding cells during an initial glucose stimulation and
284 determined what proportion of these 5 cells remained first responders during a repeated
285 glucose stimulation (Figure 3.D). Upon cytokine treatment, there was a small but non-
286 significant change in the average consistency of first responders upon repeated glucose
287 stimulation compared to untreated controls (34% vs. 38% respectively, p=0.9769) (Figure 3.E).
288 Restoration of gap junction coupling via co-treatment with S293 mimetic peptide had no impact
289 on the consistency of first responders relative to cytokine only treatment or untreated controls
290 (Figure 3.E) (p=0.8758).

291 Therefore, treatment with pro-inflammatory cytokines reduced the coordination of the
292 first phase [Ca^{2+}] response. Restoration of gap junction coupling does not provide any recovery
293 of first-responder cells, nor the coordination of the first phase [Ca^{2+}] response.

294

295 *Restoration of gap junction coupling provides a partial recovery to the cytokine-mediated*
296 *disruption of highly connected β-cell hubs:* Finally, we examined the impact of pro-inflammatory
297 cytokines and the restoration of gap junction coupling on highly connected β-cell hubs. β-cell
298 hubs have been demonstrated to maintain coordinated [Ca^{2+}] dynamics and are distinct from
299 first responder cells [25,28,29]. Importantly previous work indicated a decrease in β-cell hubs
300 upon diabetogenic conditions [13,29]. Following Ca^{2+} imaging we analyzed individual cell time-

courses and formed a functional network and identified the most highly connected cells as β-cell hubs (Figure 4.A, see Methods). In control islets the number of highly synchronized functional connections and highly synchronized hubs was high and consistent with prior measurements [29,30]. Upon treatment with pro-inflammatory cytokines for 1 hour, there was no significant impact the mean degree of correlation (Figure 4.A-B). However following treatment with pro-inflammatory cytokines for 24 hours, there was a significant decrease in the mean degree of correlation ($p = 0.0375$, Figure 4. A-C). There was also a decrease in proportion of highly synchronized functional connections or "links" ($p=0.0750$, Figure 4.D) and highly connected β-cell hubs ($p = 0.2087$, Figure 4.E). Co-treatment with S293 peptide did not show a significant change in either functional connections or β-cell hubs compared to cytokines alone (Figure 4.D,E). This indicates that restoration of gap junction coupling was not sufficient to recover highly synchronized functional connections and highly connected β-cell hubs. S293 peptide alone showed similar functional connections and β-cell hubs as untreated controls. Under 1 hour cytokine treatment, co-treatment with S293 had no impact (Supplemental 2).

Similar to our analysis of first-responder cell consistency, an average of ~50% of β-cell hubs remained as hubs following repeated glucose stimulation (Figure 4.F). We tested whether this consistency is affected by both pro-inflammatory cytokines and restoration of gap junction coupling. Upon cytokine treatment, there was a decrease in the consistency of hubs (~32%) compared to untreated control islets (~53%). Restoration of gap junction coupling via co-treatment with S293 mimetic peptide showed a trend to improved the consistency of hubs compared to cytokine treatment alone (~67% vs ~32%, $p=0.4285$, Figure 4.G), with similar measurements to S293 peptide treatment alone, albeit lacking statistical significance.

Therefore, treatment with pro-inflammatory cytokines reduced the presence of highly synchronized functional connections and β-cell hubs. Restoration of gap junction coupling and islet-wide synchronization has little influence on hubs but maintains the consistency of those remaining hub cells.

328 ***Discussion***

329 Cx36 gap junctions have previously been identified as an important regulator of β-cell
330 coordination and islet function through the electrical coupling of neighboring β-cells.
331 Pharmacological or genetic improvements in Cx36 gap junctions has been shown to recover
332 [Ca^{2+}] and insulin secretion responses in models of diabetes invitro, and delay onset of diabetes
333 in vivo, indicating a protective role that gap junctions play in islet function [12,31]. Functional
334 sub-populations (which emerge as a result of β-cell heterogeneity) have been identified that
335 can drive the coordinated islet electrical response [27]. The goal of this study was to examine
336 the influence of gap junctions on functional sub-populations of β-cells in a cytokine-mediated
337 diabetogenic environment. Towards this, in the presence of a cocktail of pro-inflammatory
338 cytokines, we recovered Cx36 gap junction coupling using a mimetic peptide which we
339 previously developed [12]. We then applied both optogenetics and calcium imaging to measure
340 cell recruitment and calcium dynamics to identify and characterize three functional sub-
341 populations that have previously been described [28] including first responders and hubs. We
342 found that while gap junction coupling could be successfully recovered under pro-inflammatory
343 conditions, as indicated by FRAP, optogenetic stimulation, and/or analysis of calcium dynamics
344 revealed that functional subpopulations remained largely impaired. Thus, while Cx36 gap
345 junction coupling is critical for overall islet function, loss of cell-intrinsic properties likely drives
346 the impairment of functional sub-populations under diabetogenic conditions.
347

348 *Impairment of functional sub-populations under diabetogenic conditions:* Increased levels of
349 proinflammatory cytokines within the islet microenvironment, including IL1-β and TNF-α, is a
350 key feature of diabetes and has been attributed to driving islet dysfunction [16,32,33]. Prior
351 studies have found that functional sub-populations are also disrupted in diabetes, such as
352 reduced numbers of β-cell hubs under both pro-inflammatory cytokines and gluco-lipo-toxic
353 conditions [29],reduced consistency of wave initiator / leader cells under high-fat diet conditions
354 [15] and reduced presence of hubs and leaders in islets from human subjects with type2
355 diabetes [34]. In this study we extended these findings to show both the cells that recruit a large
356 proportion of the neighbors to show elevated [Ca^{2+}] (high-responders), and the first responder
357 cells that respond earliest to glucose were also both disrupted by pro-inflammatory cytokines.
358 This points to a general occurrence for functional sub-populations to be disrupted under
359 diabetogenic conditions. Notably, each of these functional sub-population is associated with

driving a specific aspect of islet electrical response, which were also disrupted under the pro-inflammatory cytokines. For example, β-cell hubs coordinate oscillatory dynamics across the islet, and the synchronization of these oscillations was disrupted by pro-inflammatory cytokines. Similarly, first-responders coordinate and enhance the initial first-phase response to glucose elevation and the coordination of this response is disrupted by pro-inflammatory cytokines. Thus disruption to these functional sub-populations may be contributing to islet dysfunction under diabetogenic conditions.

Influence of gap junction disruption to functional subpopulations under diabetogenic conditions: Functional sub-populations such as β-cell hubs, first-responders and those that show high ChR2-recruitment of [Ca^{2+}] all exert their influence to coordinate and recruit other β-cells via Cx36 gap junction coupling. Thus, a natural hypothesis is that pro-inflammatory cytokines disrupt these sub-populations and their action, because of diminished gap junction coupling. By using the S293 peptide mimetic we can recover functional gap junction coupling equivalent to that in control untreated islets. However, unexpectedly, we did not observe substantial recoveries in the presence and action of functional sub-populations when gap junctions were recovered: we observed only partial recovery to ChR2-recruitment, and no recovery to first responders or β-cell hubs. One simple explanation is non-specific effects of the S293 peptide, however prior studies did not observe non-specific effects on [Ca^{2+}]. These findings indicate that the disruptions to functional sub-populations under pro-inflammatory cytokines are not primarily due to disruptions to gap junction coupling.

While initially unexpected, our findings are consistent with the fact that gap junction coupling is not per se a defining feature of these sub-populations. For example, cells with high ChR2-recruitment do not show increased gap junction coupling [27], β-cell hubs do not show increased gap junction coupling [30], and first responders show lower gap junction coupling[28]. Thus, gap junction coupling does not drive the formation of these sub-populations, rather they are defined by cell-intrinsic properties such as elevated glucose metabolism or electrical differences, as well as other environmental properties such as communication with α- or δ-cells [35]. Dysfunction to these cell intrinsic properties or altered communication with α- or δ-cells is therefore likely driving their disruption. However, we note that some amount of gap junction coupling will still be required for these cells to exert their influence across the islet [3].

392 Enhancing gap junction coupling can recover islet function in diabetogenic conditions
393 [12,16,36]. This has been demonstrated via both genetic and pharmacological approaches in
394 models of diabetes invitro and invivo. While promising, our findings indicate that targeting gap
395 junction coupling alone will be insufficient to fully recover islet function, given that functional β-
396 cell sub-populations will still be disrupted. For example, caloric restriction is able to improve
397 islet dysfunction that results from a high-fat diet; yet while gap junction coupling recovered,
398 wave initiators / leaders did not [15]. Inclusion of the GLP1R agonist Exendin-4 with pro-
399 inflammatory cytokines recovered gap junction coupling and coordinated [Ca^{2+}] dynamics [37],
400 while also impacting insulin secretion pathways via cAMP signaling. Thus, ensuring intrinsic
401 factors and/or communication with α- and δ-cells are recovered will likely be required. Future
402 work should examine which of these factors is important to both define functional sub-
403 populations and preserve their action on islet function under diabetogenic conditions.
404
405 *Limitations and Future Work:* Our findings indicate that protection of gap junctions alone is not
406 sufficient to recover cytokine-mediated loss of functional subpopulations. However other
407 factors within the islet microenvironment during diabetes can also impact islet function,
408 including gluco- and lipo-toxicity, amyloid plaque formation, and other pro-inflammatory
409 cytokines such as IL6. Thus, extending our findings to other invitro treatments and mouse
410 models of diabetes will be needed in future work. Another important factor is that our study
411 examined a 24 hours treatment with pro-inflammatory cytokines and/or S293 peptide mimetic.
412 This compares to a 1-6 hour treatment time in previous studies that support the recovery of
413 gap junctions and islet function by S293 [12]. While we observed a recovery of gap junction
414 coupling, it is possible that under more acute treatments we will observe some recovery in
415 functional sub-populations and a further enhancement in gap junction coupling: Cx36 turnover
416 has a half-life of ~3 hours [38]. Nevertheless a longer term treatment is likely more reflective of
417 the islet microenvironment in diabetes.
418
419 *Summary:* Overall, in thus study we demonstrate that proinflammatory cytokines disrupt the
420 presence and action of functional β-cell sub-populations such as hubs, first responders and
421 cell-recruitment of [Ca^{2+}]. Preventing the decline in gap junction coupling was not sufficient for
422 recovering these functional β-cell sub-populations. This correlates with gap junction coupling
423 not being a factor that defines β-cell heterogeneity within the islet, and rather cell intrinsic

424 properties or other aspects of intra-islet communication instead being disrupted by the pro-
425 inflammatory environment.
426

427 ***Figure Descriptions***

428 **Figure 1.** Restoration cytokine-mediated disruptions to gap junction coupling, as measured by
429 FRAP. (A) Isolated mouse islets were treated with a 0.1x cocktail of proinflammatory cytokines
430 and co-incubated with 30 μM S293 peptide for 1 hour before imaging. (B) Representative image
431 of Rhodamine123 loaded islet pre- and post-photobleaching, along with Fluorescence
432 Recovery After Photobleaching (FRAP) time-course after photobleaching, showing
433 fluorescence recovery in the bleached region. (C) Rate of recovery was calculated as a proxy
434 for gap junction permeability in untreated, cytokine, cytokine plus S293 peptide, and S293
435 peptide alone treatments. Data represents Mean ± S.E.M. with each islet represented by a data
436 point (from 6 mice), and each measurement is normalized to the mean control value per mouse.
437 * indicates $p < 0.05$.
438

439 **Figure 2**. Impact of gap junction restoration on the cytokine-mediated disruption to ChR2-
440 mediated recruitment of [Ca^{2+}]. (A) A ChR2-expressing islet (left), where a single ChR2-YFP
441 expressing cell was stimulated at 1 Hz (i) and calcium response was recorded across the islet
442 which exhibited both regions of recruited (ii) and unrecruited (iii) cells in untreated conditions
443 (middle). The result [Ca^{2+}] activity was then quantified (right). (B) As in A, under cytokine-treated
444 conditions. (C) Histogram indicating the proportion of the islet recruited by a single cell
445 stimulation under each treatment condition. (D) Mean proportion of the islet recruited by a
446 single cell stimulation under each treatment condition. Data represents Mean ± S.E.M. with
447 each islet represented by a data point (from 15 mice). (E) The proportion of cells that were able
448 to recruit an area larger than 30% of the islet under the cytokine and S293 conditions indicated.
449 ** indicates $p < 0.01$, **** indicates $p < 0.0001$.
450

451 **Figure 3.** Impact of gap junction restoration on the cytokine-mediated disruption to the temporal
452 and spatial consistency of first responders. (A) Time-course of [Ca^{2+}] in first responder cells
453 (red) and last responder cells (green) following stimulation by high (11mM) glucose, under
454 control or cytokine-treated conditions (for 1h or 24h). (B) The mean time spread between the
455 first and last responders (ΔT) in islets treated with cytokines for 24 hours or 1 hour, compared
456 to untreated. (C) The mean time spread in islets treated for 24 hours, with cytokines and/or
457 S293 peptide recovery of gap junction coupling. (D) Time-course of [Ca^{2+}] in first responder
458 cells (red) and last responder cells (green), subjected to repeated stimulation from low to high

459 glucose (E) The percent consistency of first responders in untreated cells (~40%) or those with
460 cytokines and/or S293 peptide recovery of gap junction coupling. ** indicates $p < 0.01$, ***
461 indicates $p < 0.001$.
462
463 **Figure 4.** Impact of gap junction restoration on the cytokine-mediated disruption of highly
464 connected β-cell hubs. Representative connectivity map (above) and time-courses (below) of
465 islets under control or cytokine-treated conditions (for 1h or 24h). (B) The mean correlation
466 coefficient in islets treated with cytokines for 24 hours or 1 hour, compared to untreated. (C)
467 Mean correlation coefficient in islets treated for 24 hours, with cytokines and/or S293 peptide
468 recovery of gap junction coupling. (D) As in C for the average number of links between cells.
469 (E) As in C for the proportion of hub cells among the entire islet cell population. (F) Time-course
470 of $[Ca^{2+}]$ in β-cell hubs that are consistent or not consistent, together with representative
471 connectivity maps. (G) The percent consistency of hubs in untreated cells (>50%) or those with
472 cytokines and/or S293 peptide recovery of gap junction coupling. * indicates $p < 0.05$, **
473 indicates $p < 0.01$, *** indicates $p < 0.001$.
474
475
476 **Supplement 1.** First responder cells under 1h cytokine treatment with/without gap junction
477 restoration. (A) The mean time spread in islets treated for 1 hour, with cytokines and/or S293
478 peptide recovery of gap junction coupling. (B) The percent consistency of first responders in
479 untreated cells (~40%) or those with cytokines and/or S293 peptide recovery of gap junction
480 coupling.
481
482 **Supplement 2.** Highly connected β-cell hubs under 1h cytokine treatment with/without gap
483 junction restoration. (A) Mean correlation coefficient in islets treated for 1 hour, with cytokines
484 and/or S293 peptide recovery of gap junction coupling. (B) As in A for the average number of
485 links between cells. (C) As in A for the proportion of hub cells among the entire islet cell
486 population. (D) As in A for percent consistency of hubs.
487

488 ***References***

489 1. Federation, I.D. *Diabetes around the world in 2021*. 2022 [cited 2024.
490 2. Allagnat, F., D. Martin, D.F. Condorelli, G. Waeber, and J.-A. Haefliger, *Glucose*
491 *represses connexin36 in insulin-secreting cells.* Journal of cell science, 2005. **118**(22):
492 p. 5335-5344.
493 3. Benninger, R.K., M. Zhang, W.S. Head, L.S. Satin, and D.W. Piston, *Gap junction*
494 *coupling and calcium waves in the pancreatic islet.* Biophysical journal, 2008. **95**(11): p.
495 5048-5061.
496 4. Farnsworth, N.L., A. Hemmati, M. Pozzoli, and R.K. Benninger, *Fluorescence recovery*
497 *after photobleaching reveals regulation and distribution of connexin36 gap junction*
498 *coupling within mouse islets of Langerhans.* The Journal of physiology, 2014. **592**(20):
499 p. 4431-4446.
500 5. Ravier, M.A., M. Guldenagel, A. Charollais, A. Gjinovci, D. Caille, G. Sohl, C.B.
501 Wollheim, K. Willecke, J.-C. Henquin, and P. Meda, *Loss of connexin36 channels alters*
502 *β-cell coupling, islet synchronization of glucose-induced Ca2+ and insulin oscillations,*
503 *and basal insulin release.* Diabetes, 2005. **54**(6): p. 1798-1807.
504 6. Pipeleers, D.G., *Heterogeneity in pancreatic β-cell population.* Diabetes, 1992. **41**(7): p.
505 777-781.
506 7. Stožer, A., M. Gosak, J. Dolenšek, M. Perc, M. Marhl, M.S. Rupnik, and D. Korošak,
507 *Functional connectivity in islets of Langerhans from mouse pancreas tissue slices.* PLoS
508 computational biology, 2013. **9**(2): p. e1002923.
509 8. Benninger, R.K., W.S. Head, M. Zhang, L.S. Satin, and D.W. Piston, *Gap junctions and*
510 *other mechanisms of cell–cell communication regulate basal insulin secretion in the*
511 *pancreatic islet.* The Journal of physiology, 2011. **589**(22): p. 5453-5466.
512 9. Speier, S., A. Gjinovci, A. Charollais, P. Meda, and M. Rupnik, *Cx36-mediated coupling*
513 *reduces β-cell heterogeneity, confines the stimulating glucose concentration range, and*
514 *affects insulin release kinetics.* Diabetes, 2007. **56**(4): p. 1078-1086.
515 10. Head, W.S., M.L. Orseth, C.S. Nunemaker, L.S. Satin, D.W. Piston, and R.K. Benninger,
516 *Connexin-36 gap junctions regulate in vivo first-and second-phase insulin secretion*
517 *dynamics and glucose tolerance in the conscious mouse.* Diabetes, 2012. **61**(7): p.
518 1700-1707.
519 11. Hodson, D.J., R.K. Mitchell, E.A. Bellomo, G. Sun, L. Vinet, P. Meda, D. Li, W.-H. Li, M.
520 Bugliani, and P. Marchetti, *Lipotoxicity disrupts incretin-regulated human β cell*
521 *connectivity.* The Journal of clinical investigation, 2013. **123**(10): p. 4182-4194.
522 12. St. Clair, J.R., M.J. Westacott, J. Miranda, N.L. Farnsworth, V. Kravets, W.E. Schleicher,
523 J.M. Dwulet, C.H. Levitt, A. Heintz, and N.W. Ludin, *Restoring connexin-36 function in*
524 *diabetogenic environments precludes mouse and human islet dysfunction.* The Journal
525 of Physiology, 2023. **601**(18): p. 4053-4072.
526 13. Farnsworth, N.L., R.L. Walter, A. Hemmati, M.J. Westacott, and R.K. Benninger, *Low*
527 *level pro-inflammatory cytokines decrease connexin36 gap junction coupling in mouse*
528 *and human islets through nitric oxide-mediated protein kinase Cδ.* Journal of Biological
529 Chemistry, 2016. **291**(7): p. 3184-3196.
530 14. Carvalho, C.d.F., R.B. Oliveira, A. Britan, J. Santos-Silva, A.C. Boschero, P. Meda, and
531 C.B. Collares-Buzato, *Impaired β-cell-β-cell coupling mediated by Cx36 gap junctions in*
532 *prediabetic mice.* American Journal of Physiology-Endocrinology and Metabolism, 2012.
533 **303**(1): p. E144-E151.
534 15. Corezola do Amaral, M.E., V. Kravets, J.M. Dwulet, N.L. Farnsworth, R. Piscopio, W.E.
535 Schleicher, J.G. Miranda, and R.K. Benninger, *Caloric restriction recovers impaired β-*

cell-β-cell gap junction coupling, calcium oscillation coordination, and insulin secretion in prediabetic mice. American Journal of Physiology-Endocrinology and Metabolism, 2020. **319**(4): p. E709-E720.

16. Farnsworth, N.L., R.A. Piscopio, and R.K. Benninger, *Modulation of gap junction coupling within the islet of langerhans during the development of type 1 diabetes.* Frontiers in Physiology, 2022. **13**: p. 913611.
17. Westacott, M.J., N.L. Farnsworth, J.R. St. Clair, G. Poffenberger, A. Heintz, N.W. Ludin, N.J. Hart, A.C. Powers, and R.K. Benninger, *Age-dependent decline in the coordinated [Ca2+] and insulin secretory dynamics in human pancreatic islets.* Diabetes, 2017. **66**(9): p. 2436-2445.
18. Ravier, M., J. Sehlin, and J. Henquin, *Disorganization of cytoplasmic Ca 2+ oscillations and pulsatile insulin secretion in islets from ob/ob mice.* Diabetologia, 2002. **45**: p. 1154-1163.
19. Heimberg, H., A. De Vos, A. Vandercammen, E. Van Schaftingen, D. Pipeleers, and F. Schuit, *Heterogeneity in glucose sensitivity among pancreatic beta-cells is correlated to differences in glucose phosphorylation rather than glucose transport.* The EMBO journal, 1993. **12**(7): p. 2873-2879.
20. Roscioni, S.S., A. Migliorini, M. Gegg, and H. Lickert, *Impact of islet architecture on β-cell heterogeneity, plasticity and function.* Nature Reviews Endocrinology, 2016. **12**(12): p. 695-709.
21. Wang, Y.J., J. Schug, K.-J. Won, C. Liu, A. Naji, D. Avrahami, M.L. Golson, and K.H. Kaestner, *Single-cell transcriptomics of the human endocrine pancreas.* Diabetes, 2016. **65**(10): p. 3028-3038.
22. Wojtusciszyn, A., M. Armanet, P. Morel, T. Berney, and D. Bosco, *Insulin secretion from human beta cells is heterogeneous and dependent on cell-to-cell contacts.* Diabetologia, 2008. **51**: p. 1843-1852.
23. Benninger, R.K., T. Hutchens, W.S. Head, M.J. McCaughey, M. Zhang, S.J. Le Marchand, L.S. Satin, and D.W. Piston, *Intrinsic islet heterogeneity and gap junction coupling determine spatiotemporal Ca2+ wave dynamics.* Biophysical journal, 2014. **107**(11): p. 2723-2733.
24. Giordano, E., D. Bosco, V. Cirulli, and P. Meda, *Repeated glucose stimulation reveals distinct and lasting secretion patterns of individual rat pancreatic B cells.* The Journal of clinical investigation, 1991. **87**(6): p. 2178-2185.
25. Benninger, R.K. and V. Kravets, *The physiological role of β-cell heterogeneity in pancreatic islet function.* Nature Reviews Endocrinology, 2022. **18**(1): p. 9-22.
26. Rutter, G.A., A. Gresch, L. Delgadillo Silva, and R.K. Benninger, *Exploring pancreatic beta-cell subgroups and their connectivity.* Nature metabolism, 2024: p. 1-15.
27. Westacott, M.J., N.W. Ludin, and R.K. Benninger, *Spatially organized β-cell subpopulations control electrical dynamics across islets of Langerhans.* Biophysical journal, 2017. **113**(5): p. 1093-1108.
28. Kravets, V., J.M. Dwulet, W.E. Schleicher, D.J. Hodson, A.M. Davis, L. Pyle, R.A. Piscopio, M. Sticco-Ivins, and R.K. Benninger, *Functional architecture of pancreatic islets identifies a population of first responder cells that drive the first-phase calcium response.* PLoS Biology, 2022. **20**(9): p. e3001761.
29. Johnston, N.R., R.K. Mitchell, E. Haythorne, M.P. Pessoa, F. Semplici, J. Ferrer, L. Piemonti, P. Marchetti, M. Bugliani, and D. Bosco, *Beta cell hubs dictate pancreatic islet responses to glucose.* Cell metabolism, 2016. **24**(3): p. 389-401.

30. Briggs, J.K., A. Gresch, I. Marinelli, J.M. Dwulet, D.J. Albers, V. Kravets, and R.K. Benninger, *β-cell intrinsic dynamics rather than gap junction structure dictates subpopulations in the islet functional network.* Elife, 2023. **12**: p. e83147.
31. Farnsworth, N.L., R.A. Piscopio, W.E. Schleicher, D.G. Ramirez, J.G. Miranda, and R.K. Benninger, *Modulation of gap junction coupling within the islet of langerhans during the development of type 1 diabetes.* Frontiers in Physiology, 2022. **13**: p. 913611.
32. Akash, M.S.H., K. Rehman, and S. Chen, *Role of inflammatory mechanisms in pathogenesis of type 2 diabetes mellitus.* Journal of cellular biochemistry, 2013. **114**(3): p. 525-531.
33. Alexandraki, K., C. Piperi, C. Kalofoutis, J. Singh, A. Alaveras, and A. Kalofoutis, *Inflammatory process in type 2 diabetes: The role of cytokines.* Annals of the New York Academy of Sciences, 2006. **1084**(1): p. 89-117.
34. Gosak, M., R. Yan-Do, H. Lin, P.E. MacDonald, and A. Stožer, *Ca2+ oscillations, waves, and networks in islets from human donors with and without type 2 diabetes.* Diabetes, 2022. **71**(12): p. 2584-2596.
35. Jin, E., J.K. Briggs, R.K. Benninger, and M.J. Merrins, *Glucokinase activity controls subpopulations of β-cells that alternately lead islet Ca2+ oscillations.* bioRxiv, 2024.
36. Klee, P., F. Allagnat, H. Pontes, M. Cederroth, A. Charollais, D. Caille, A. Britan, J.-A. Haefliger, and P. Meda, *Connexins protect mouse pancreatic β cells against apoptosis.* The Journal of clinical investigation, 2011. **121**(12): p. 4870-4879.
37. Farnsworth, N.L., R. Walter, R.A. Piscopio, W.E. Schleicher, and R.K. Benninger, *Exendin-4 overcomes cytokine-induced decreases in gap junction coupling via protein kinase A and Epac2 in mouse and human islets.* The Journal of physiology, 2019. **597**(2): p. 431-447.
38. Wang, H.Y., Y.-P. Lin, C.K. Mitchell, S. Ram, and J. O'Brien, *Two-color fluorescent analysis of connexin 36 turnover: relationship to functional plasticity.* Journal of cell science, 2015. **128**(21): p. 3888-3897.

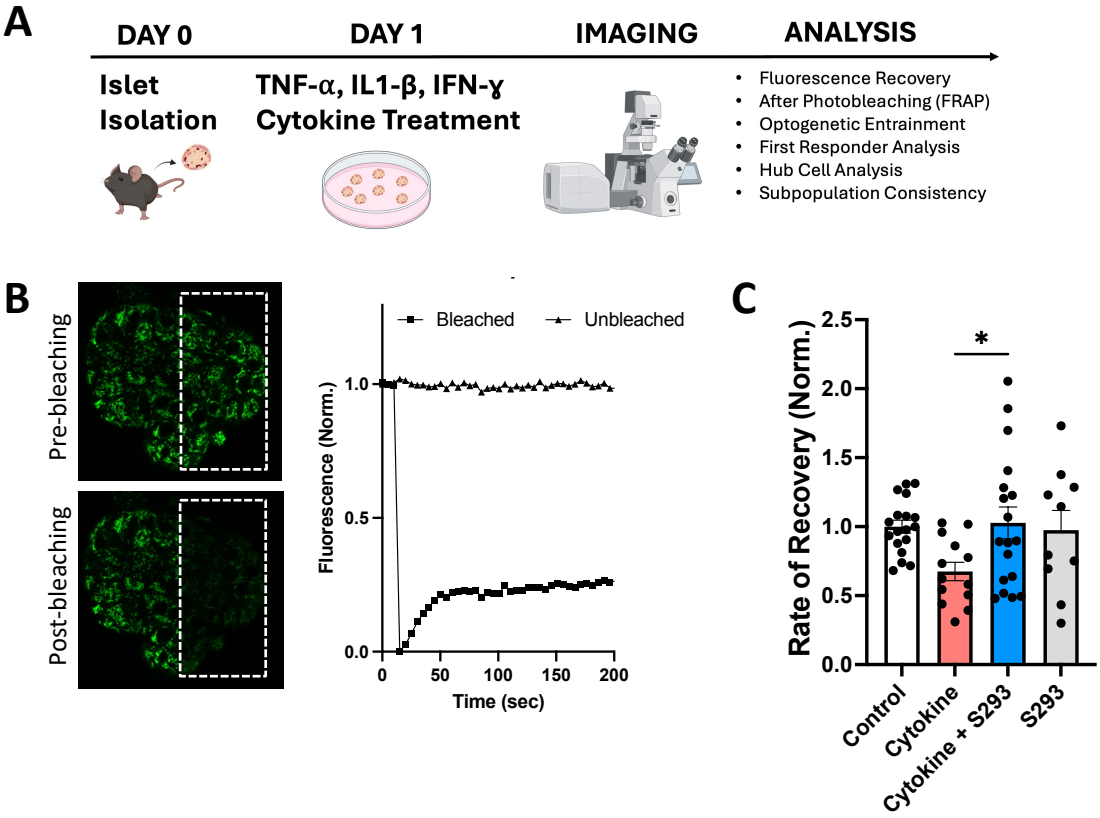
A
DAY 0
DAY 1
IMAGING
ANALYSIS
Islet Isolation
TNF-α, IL1-β, IFN-γ Cytokine Treatment
Fluorescence Recovery
After Photobleaching (FRAP)
Optogenetic Entrainment
First Responder Analysis
Hub Cell Analysis
Subpopulation Consistency
B
Pre-bleaching
Post-bleaching
Bleached
Unbleached
Fluorescence (Norm.)
Time (sec)
C
Rate of Recovery (Norm.)
Control
Cytokine
Cytokine + S293
S293

Figure 1

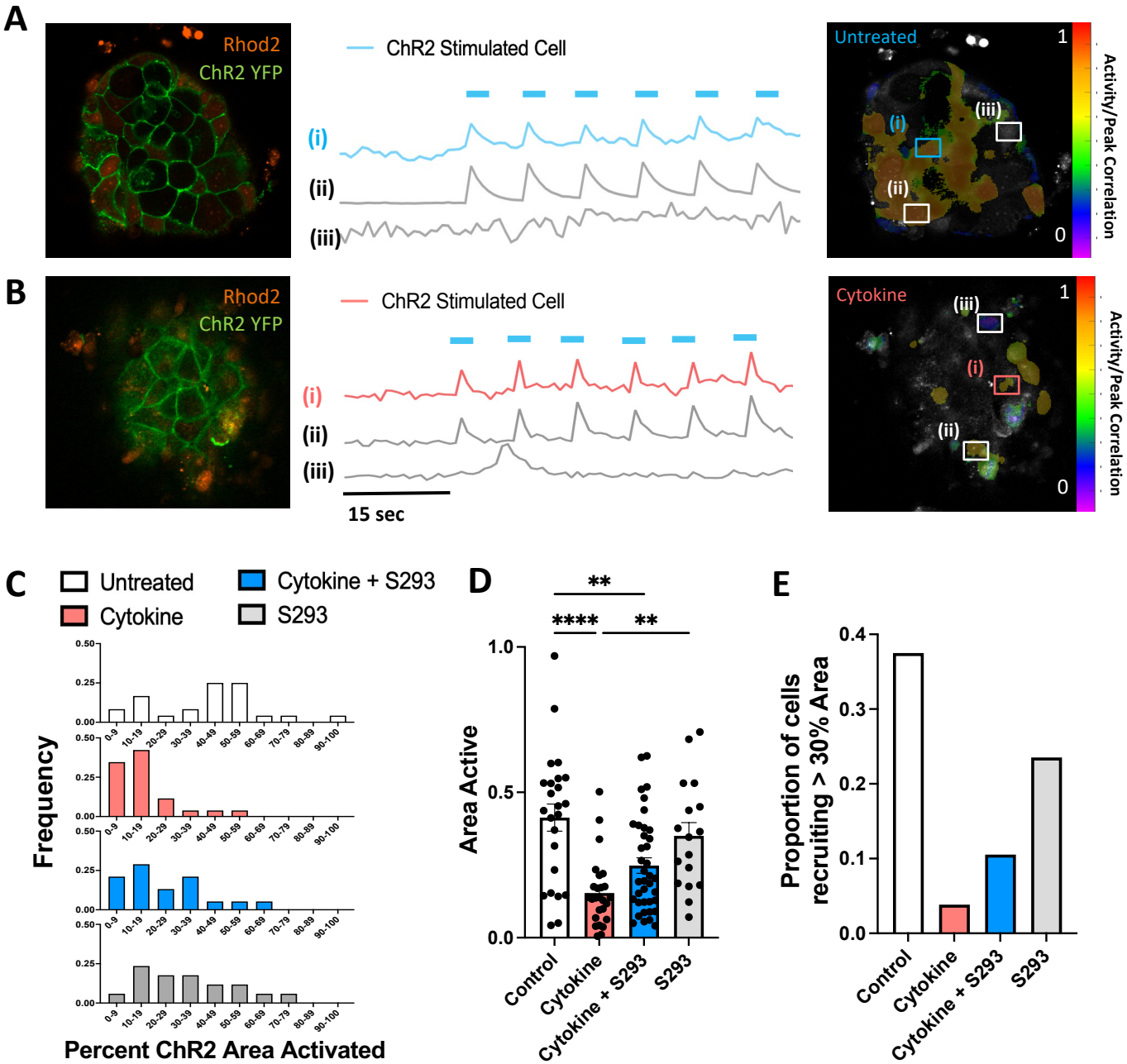
A
Rhod2
ChR2 YFP
ChR2 Stimulated Cell
(i)
(ii)
(iii)
Untreated
1
0
Activity/Peak Correlation
B
Rhod2
ChR2 YFP
ChR2 Stimulated Cell
(i)
(ii)
(iii)
15 sec
Cytokine
1
0
Activity/Peak Correlation
C
Untreated
Cytokine
Cytokine + S293
S293
Frequency
0.50
0.25
0.00
0-9
10-19
20-29
30-39
40-49
50-59
60-69
70-79
80-89
90-100
Percent ChR2 Area Activated
D
**
****
**
Area Active
1.0
0.5
0.0
Control
Cytokine
Cytokine + S293
S293
E
Proportion of cells recruiting > 30% Area
0.4
0.3
0.2
0.1
0.0
Control
Cytokine
Cytokine + S293
S293

Figure 2

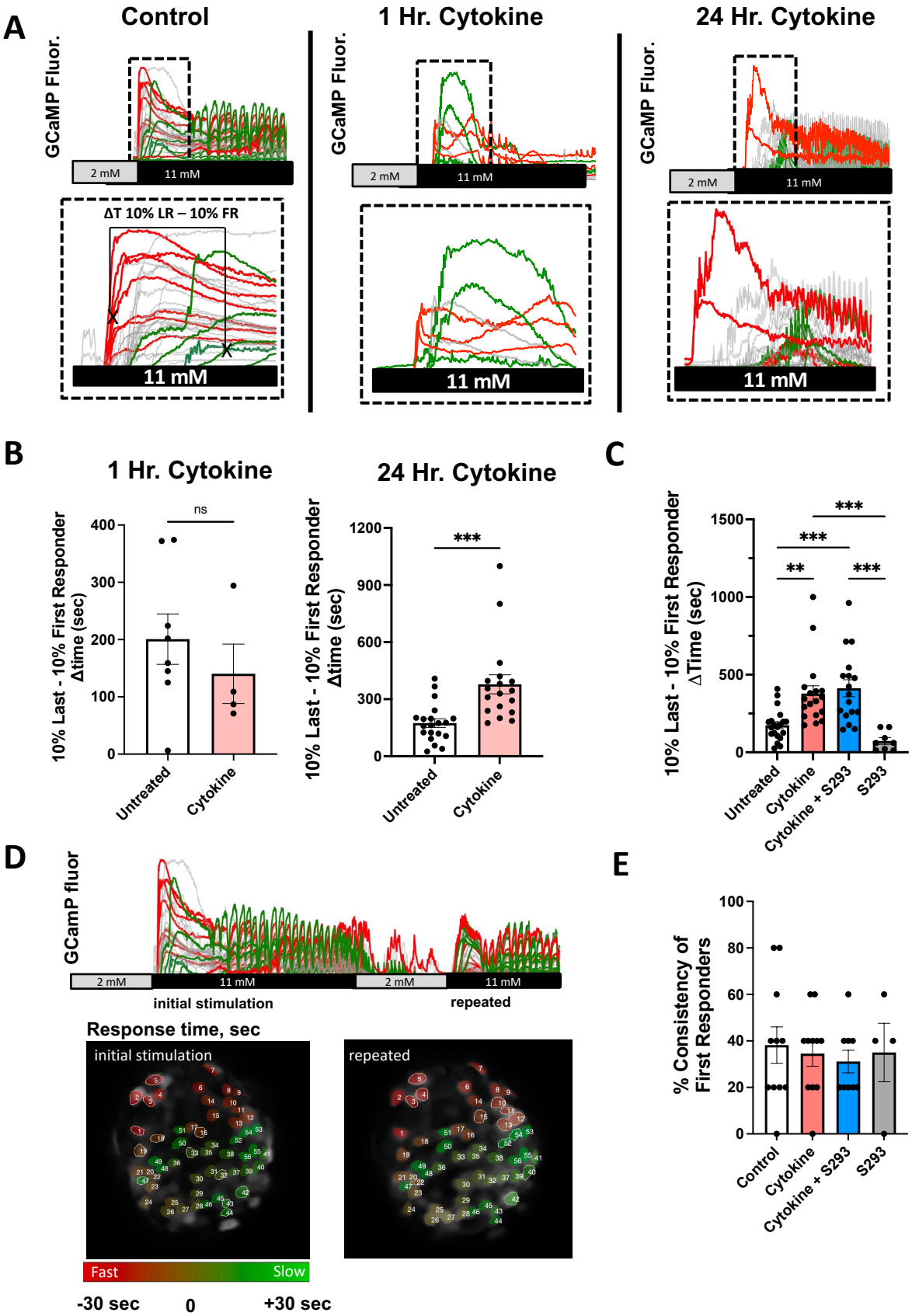
A
Control
1 Hr. Cytokine
24 Hr. Cytokine
GCaMP Fluor.
2 mM
11 mM
ΔT 10% LR – 10% FR
B
1 Hr. Cytokine
24 Hr. Cytokine
10% Last - 10% First Responder Δtime (sec)
ns
***
Untreated
Cytokine
C
10% Last - 10% First Responder ΔTime (sec)
**
Cytokine + S293
S293
D
GCamP fluor
initial stimulation
repeated
Response time, sec
Fast
Slow
-30 sec
0
+30 sec
E
% Consistency of First Responders
Control

Figure 3

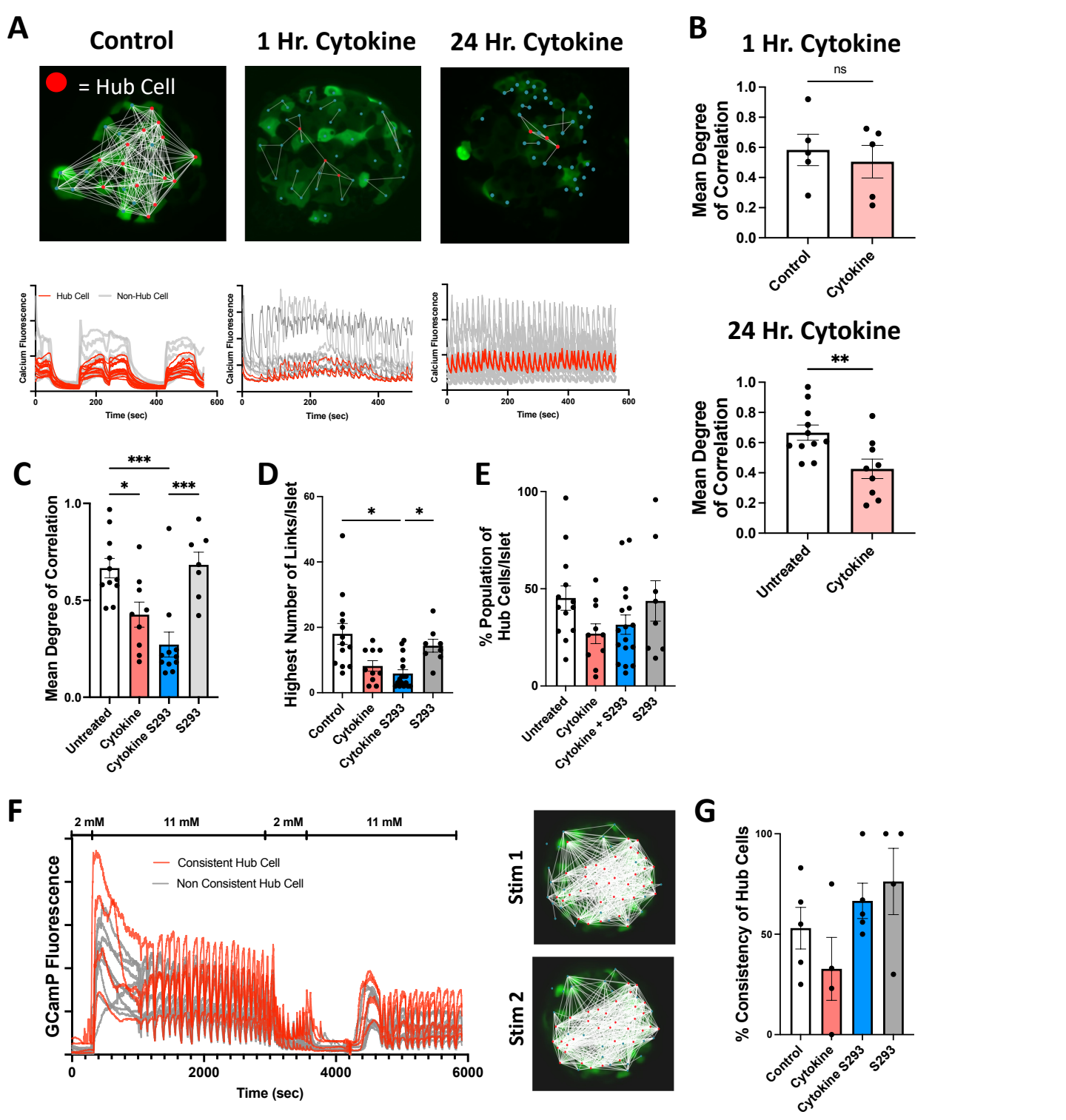
A
Control
1 Hr. Cytokine
24 Hr. Cytokine
= Hub Cell
Hub Cell
Non-Hub Cell
Calcium Fluorescence
Time (sec)
B
1 Hr. Cytokine
ns
Mean Degree of Correlation
Control
Cytokine
24 Hr. Cytokine
**
Untreated
Cytokine
C
***
*
Mean Degree of Correlation
Untreated
Cytokine
Cytokine S293
S293
D
Highest Number of Links/Islet
Control
Cytokine
Cytokine S293
S293
E
% Population of Hub Cells/Islet
Untreated
Cytokine
Cytokine + S293
S293
F
2 mM
11 mM
2 mM
11 mM
Consistent Hub Cell
Non Consistent Hub Cell
GCamP Fluorescence
Time (sec)
Stim 1
Stim 2
G
% Consistency of Hub Cells
Control
Cytokine
Cytokine S293
S293

Figure 4

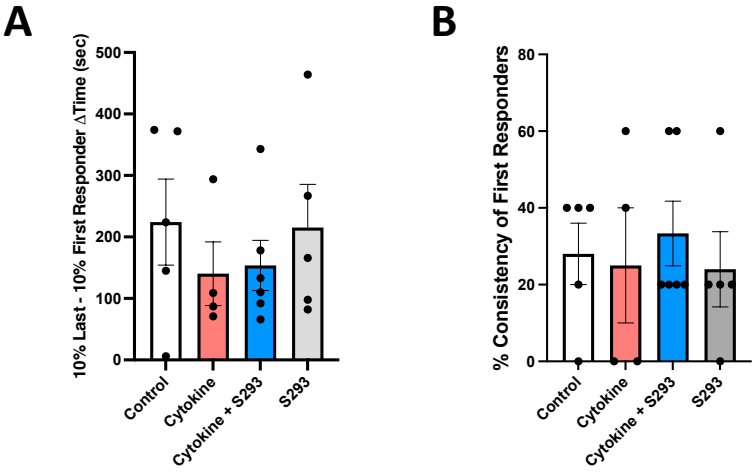

Supplement 1

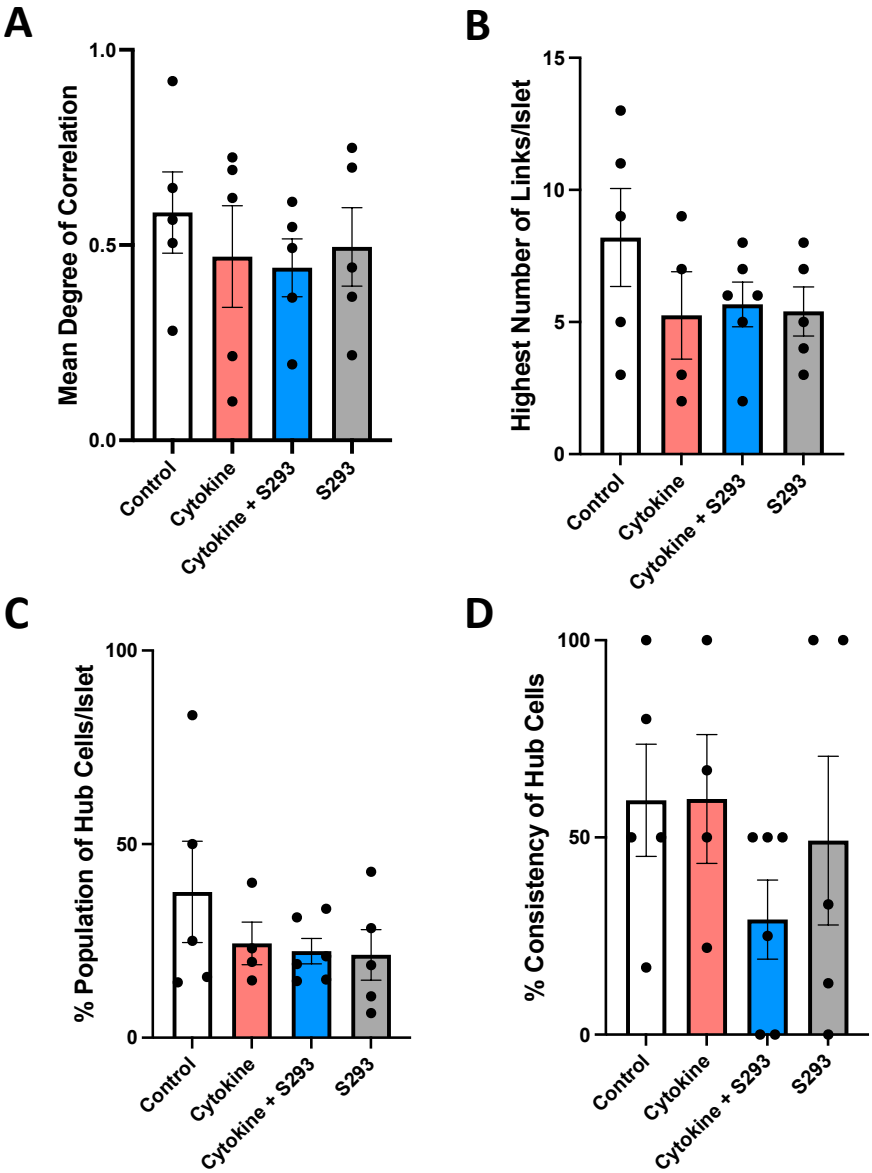

Supplement 2